Research Article

EFFECT OF ACTIVATION ENERGY, NEWTONIAN COOLING FLOW OF NANOFLUID PAST A STRETCHING SHEET WITH VARIABLE VISCOSITY INSPIRED BY THERMAL RADIATION

Dr. Y. Madhusudhana Reddy

Dept of Mathematics, Sri Venkateswara Degree & PG College, Anantapur, Andhrapradesh-515001

ABSTRACT

We analyze the combined influence of activation energy,Brownian motion,thermophopresis, past a stretching sheet with variable viscosity and thermal radiation. The governing equations have been solved by employing fifth-order Runge-Kutta-Fehlberg method along with shooting technique. The effects of various parameterson the velocity, temperature and concentration as well as on the local skin-friction coefficient, local Nusselt number and local Sherwood number are presented graphically and discussed. It is observed that a velocities components increase with Hall parameter(m), Brownian motion parameter(Nb), Radiation parameter(Rd), Viscosity parameter (□r), Convective heat transfer constant(h1), reduces with thermophoresis parameter(Nt). Nusselt number increase in □r and reduces Nu and Sh, increase in □r/h1 reduces rate of heat transfer and enhances mass transfer.

Keywords: Activation energy,Brownian motion, Thermophoresis, Stretching surface, variable viscosity, thermal radiation, Newtonian cooling.

INTRODUCTION

The word “nanofluid” coined by Choi [9] refers to a liquid suspension containing ultra - fine particles (diameter less than 50 nm). The traditional fluids viz.,water, mineral oils, ethylene glycol, engine oil with limited heat transfer capabilities are used for heat transfer applications. It has been pointed that contribution of Brownian motion is much lower than other factors such as size effect, clustering of nanoparticles and surface adsorption. The different theories explaining the enhanced heat transfer characteristics of nanofluids have been evaluated by Buongiorno [7]. He developed an analytical model for convective transport in nanofluids which takes into account the Brownian diffusion and thermophoresis.

Anjali Devi and Mekala [5] have analysed discussed the Role of Brownian Motion and Thermophoresis Effects on Hydromagnetic Flow of Nanofluid over a Nonlinearly Stretching Sheet with Slip effects and Solar Radiation. Dulal Pal et al [11] have briefly discussed the thermophoresis and Brownian motion effects on magneto-convective heat transfer of viscoelastic nanofluid over a stretching sheet with nonlinear thermal radiation. Falana et al. [12] have been described the effect of Brownian Motion and Thermophoresis on a Nonlinearly Stretching Permeable Sheet in a Nanofluid.KempannagariAnantha Kumar et al. [16]discussedthe thermophoresis and brownian motion effects on mhdmicropolarnanofluid flow past a stretching surface with non-uniform heat source/sink.Mabood et al. [18] haveobserved the Framing the features of Brownian motion and thermophoresis on radiative nanofluid flow past a rotating stretching sheet with magnetohydrodynamics.Shobha and PatilMallikarjun [29] demonstrated the fully developed mixed convection in a vertical channel filled with nanofluids with heat source or sink

The effect of temperature-dependent viscosity on heat and mass transfer laminar boundary layer flow has been discussed by many authors (Mukhopadhyay and Layek [20], Ali [3], Makinde [19], Prasad et al. [24], Alamet al. [2]) in various situations. They showed that when this effect was included, the flow characteristics might change substantially compared with the constant viscosity assumption. Salem [26] investigated variable viscosity and thermal conductivity effects on MHD flow and heat transfer in viscoelastic fluid over a stretching sheet. Xi-Yan Tian et al. [31] investigated the 2D boundary layer flow and heat transfer in variable viscosity MHD flow over a stretching plate.

Hall currents are important and they have a marked effect on the magnitude and direction of the current density and consequently on the magnetic force term. The problem of MHD free convection flow with Hall currents has many important engineering applications such as in power generators, MHD accelerators, refrigeration coils, transmission lines, electric transformers, heating elements etc., Watanabe and Pop [30], Abo-Eldahab and Salem [1]], Ranaet al. [25], Shit [28],Gnanaprasunambe et al[14] among others have advanced studies on Hall effect on MHD past stretching sheet. Chamkhaet al [8] analyzed the unsteady MHD free convective heat and mass transfer from a vertical porous plate with Hall current, thermal radiation and chemical reaction effects. Recently, Gnanaprsunamba [13] has discussed the effect of Brownian motion, thermophoresis and thermal radiation on hydromagnetic heat and mass transfer flow of nanofluid past a stretching sheet.

The activation energy is demarcated as the least amount of energy that reactants should acquire before involving in the chemical reaction. The chemical reaction along with activation energy has important applications in food processing, chemical engineering geothermal reservoirs, and oil emulsions. Krishna et al. [17] explored the hall effects on MHD convection chemical reactions with finite Arrhenius activation energy. Convective flows of a second-grade rotating fluid in porous medium. Netai Roy and Dulal Pal [22], Zahir et al [32] have studied influence of Activation Energy and Radiative MHD Casson Nanofluid Flow, Nonlinear Thermal Radiation with Ohmic Dissipation on Heat and Mass Transfer of a Casson Nanofluid Over Stretching Sheet. Recently, Amitosh Tiwari et al [4] have been discussion to activation energy impacts on hydromagnetic convective heat transfer flow of nanofluid past a surface of vertical wavy with variable properties. Kathyani and Subramanyam [15] have explored the effect of activation energy on thermally radiative, dissipative electrically conducting, viscous fluid flow in a vertical channel in the presence of heat sources. Several authors (Satya Narayana and Ramakrishna [27], Nagasasikala[21], Devasena[10] have demonstrated the influence of activation energy on flow phenomenon.

Motivated by the above-mentioned researchers, this paper aims at studying the combined influence of activation energy, Brownian motion, thermophoresis past a stretching surface with variable viscosity and thermal radiation. The governing equations have been solved by employing fifth order Runge-Kutta-Fehlberg method along with shooting technique. The effects of various parameters on the velocity, temperature and nano concentration as well as on the local skin-friction coefficient, local Nusselt number and local Sherwood number are presented graphically and discussed.

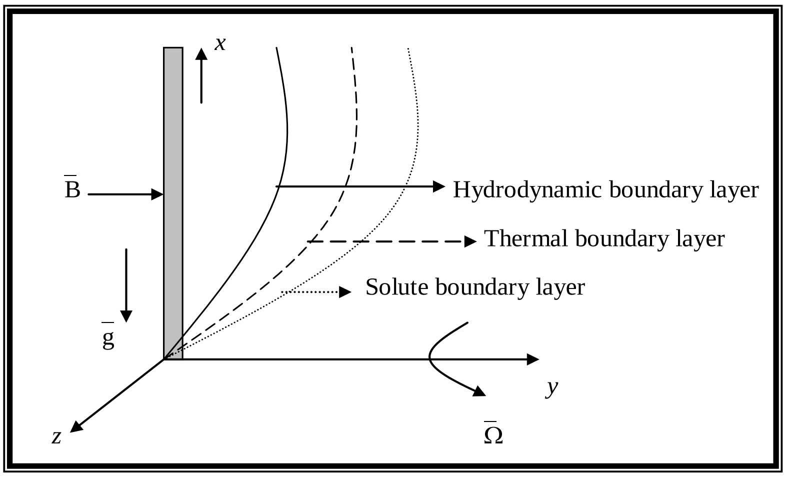

Figure 1. Physical System and Geometry of the Problem

2. FORMULATION OF THE PROBLEM

We consider the steady free-convective flow, heat and mass transfer of an incompressible, viscous and electrically conducting fluid past a stretching sheet and the sheet is stretched with a velocity proportional to the distance from a fixed origin O (Fig. 1).

The fluid viscosity μ_f is assumed to vary as a reciprocal of a linear function of temperature given by

$$\frac{1}{\mu_f} = \frac{1}{\mu_\infty}[1+\gamma_0(T-T_\infty)] \qquad (1)$$

$$\frac{1}{\mu_\infty} = a(T-T_\infty) \qquad (2)$$

Where $a = \frac{\gamma_0}{\mu_\infty}$ and $T_r = T_\infty - \frac{1}{\gamma_0}$

In the above equation both a and T_r are constants, and their values depend on the thermal property of the fluid, i.e., γ_0. In general $a> 0$ represent for liquids, whereas for gases $a< 0$.

The boundary layer free-convection flow with mass transfer and generalized Ohm's law with Hall current effect are governed by the following system of equations:

$$\frac{\partial u}{\partial x}+\frac{\partial v}{\partial y}=0 \quad (3)$$

$$\rho_f\left(u\frac{\partial u}{\partial x}+v\frac{\partial u}{\partial y}\right)=\mu_f\frac{\partial^2 u}{\partial y^2}+g(1-C_\infty)\rho_{f_\infty}\beta g(T-T_\infty)-$$
$$-(\rho_p-\rho_{f_\infty})kg(C-C_\infty)-\frac{\sigma_{nf}B_0^2}{1+m^2}(u+mw) \quad (4)$$

$$\rho_f\left(u\frac{\partial w}{\partial x}+v\frac{\partial w}{\partial y}\right)=\mu_f\frac{\partial^2 w}{\partial y^2}+\frac{\sigma_{nf}B_0^2}{1+m^2}(mu-w) \quad (5)$$

$$(\rho C_p)_f\left(u\frac{\partial T}{\partial x}+v\frac{\partial T}{\partial y}\right)=k_{rf}\frac{\partial^2 T}{\partial y^2}+\tau\{D_B(\frac{\partial T}{\partial x}\frac{\partial C}{\partial x}+\frac{\partial T}{\partial y}\frac{\partial C}{\partial y})+$$
$$+\frac{D_T}{T_\infty}((\frac{\partial T}{\partial y})^2+(\frac{\partial T}{\partial y})^2)]-\frac{\partial(q_R)}{\partial y} \quad (6)$$

$$u\frac{\partial C}{\partial x}+v\frac{\partial C}{\partial y}=D_B\frac{\partial^2 C}{\partial y^2}-k_0\left(C-C_\infty\right)(\frac{T}{T_\infty})^n Exp(-\frac{E_a}{KT})+\frac{D_T}{T_\infty}\frac{\partial^2 T}{\partial y^2} \quad (7)$$

where (u,v,w) are the velocity components along the (x,y,z) directions respectively. σ is the effective electrical conductivity, (β) is the effective thermal volumetric coefficient of expansion, $k_o$is the chemical reaction coefficient , D_B is the solution diffusivity of the medium, K_T is the thermal diffusion ratio, C_s is the concentration susceptibility, C_p is the specific heat at constant pressure , T_∞ is the mean fluid temperature and $q_R$is the radiative heat flux. $m=\frac{\sigma B_o}{en_c}$ is the Hall parameter.Ea is the activation energy coefficient.

The boundary conditions for the present problem can be written as

$u = bx,\ v = w = 0,\ -k_f\frac{\partial T}{\partial y}=h_f(Tw-T),\ C = C_w$ at $y=0$ (8)

$u\to 0,\ w\to 0,\ T\to T_\infty,\ C\to C_\infty$ at $y\to\infty$ (9)

where b (> 0) being stretching rate of the sheet. The boundary conditions on velocity in Equation(8) are the no-slip condition at the surface $y = 0$, while the boundary conditions on velocity at $y\to\infty$ follow from the fact that there is no flow far away from the stretching surface.

The radiation heat term(Brewster[6]) by using The Rosseland approximation is given by

$$q_r=-\frac{4\sigma^\bullet}{3\beta_R}\frac{\partial T'^4}{\partial y} \quad (10)$$

$$T'^4\cong 4TT_\infty^3-3T_\infty^4 \quad (11)$$

$$\frac{\partial q_R}{\partial z}=-\frac{16\sigma^\bullet T_\infty^3}{3\beta_R}\frac{\partial^2 T}{\partial y^2} \quad (12)$$

where $\sigma^\bullet$ is the Stefan –Boltzman constant and β_R is the mean absorption constant.

To examine the flow regime adjacent to the sheet, the following transformations are invoked

$$u=bxf'(\eta);v=-\sqrt{bv}\,f(\eta);w=bxg(\eta);\ \eta=\sqrt{\frac{b}{v}}\,y;\theta(\eta)=\frac{T-T_\infty}{T_w-T_\infty};\phi=\frac{C-C_\infty}{C_w-C_\infty} \quad (13)$$

where f is a dimensionless stream function, h is the similarity space variable, θ and ϕ are the dimensionless temperature and concentration respectively. Clearly, the continuity Eq. (3) is satisfied by u and v defined in Eq. (9), Substituting Eq. (10) the Eqs. (4)-(7) reduce to

$$\left(\frac{\theta-\theta_r}{\theta_r}\right)(f'-f\quad f'')+f'''-\left(\frac{\theta'}{\theta-\theta_r}\right)f''- \left(\frac{\theta-\theta_r}{\theta_r}\right)G(\theta-N\phi)+M^2\left(\frac{\theta'-\theta_r}{\theta_r}\right)\left(\frac{f'+mg}{1+m^2}\right)=0 \quad (14)$$

$$\left(\frac{\theta-\theta_r}{\theta_r}\right)(f'g-fg')+g''-\left(\frac{\theta'}{\theta-\theta_r}\right)g'-M^2\left(\frac{\theta-\theta_r}{\theta_r}\right)\left(\frac{mf'+g}{1+m^2}\right)=0 \quad (15)$$

$$(1+\frac{4Rd}{3})\theta''+Nb(\frac{\partial\theta}{\partial\overline{x}}\frac{\partial\phi^\bullet}{\partial\overline{y}}+\frac{\partial\theta}{\partial\overline{y}}\frac{\partial\phi^\bullet}{\partial\overline{x}})+Nt(\frac{\partial\theta}{\partial y})^2)=0 \quad (16)$$

$$\frac{1}{Le}\phi''-(f\phi'-\gamma\phi(1+n\delta\theta)\,\mathrm{Exp}(-\frac{E_1}{1+\delta\theta}))+(\frac{Nt}{Nb})(\theta'')=0 \quad (17)$$

Similarly, the transformed boundary conditions are given by

$f'(\eta)=1, f(\eta)=0, g(\eta)=0$ $\theta'(0)=-h_1(1-\theta(0))$,$\theta(\eta)=-h1(1-\theta(0))$,$\phi(\eta)=1$at $\eta=0$(18)

$f'(\eta)\to 0,\ g(\eta)\to 0,\ \theta(\eta)\to 0,\ \phi(\eta)\to 0$ at $\eta\to\infty$(19)

where a prime denotes the differentiation with respect to η only and the dimensionless parameters appearing in the Eqs. (13)-(17) are respectively defined as $\theta_r=\frac{T_r-T_\infty}{T_w-T_\infty}=-\left[\frac{1}{\gamma_0(T_w-T_\infty)}\right]$ the viscosity parameter, $M=\frac{\sigma B_0^2}{P_\infty b}$ the magnetic parameter, $P_r=\frac{\rho C_p \nu}{k_f}$ the Prandtl number, $\gamma=\frac{k_0}{b}(C_w-C_\infty)$ the non-dimensional chemical reaction parameter, $G=\frac{g_0\beta\ (T_w-T_\infty)}{b^2 x}$ the local Grashof number, $N=\frac{(\rho_p-\rho_{f\infty})(C_w-C_\infty)}{\rho_{f\infty}(1-C_\infty)(T_w-T_\infty)}$ the Buoyancy ratio, $Rd=\frac{4T_\infty^{\ 3}\sigma^*}{k_f\beta_R}$ the thermal radiation parameter, $Le=\frac{\mu_f}{\rho_\infty D_m}$ the Lewis number , $N_b=\frac{\tau D_B(C_w-C_\infty)}{a}$ Brownian motion parameter, $N_t=\frac{\tau D_T(T_w-T_\infty)}{aT_\infty}$ Thermophoresis parameter. $h_1=(\frac{h_f}{k_f})\sqrt{\frac{\nu}{b}}$ is convective heat transfer constant. $E_1=\frac{E_a}{KT_\infty}$ is the activation energy parameter, $\theta_w=\frac{T}{T_w},\delta=\theta_w-1$ is the temperature difference ratio.

3. METHOD OF SOLUTION

The coupled ordinary differential equations (13)-(17) are of third-order in f, and second-order in g, θ and f which have been reduced to a system of nine simultaneous equations of first-order for nine unknowns. In order to solve this system of equations numerically we require nine initial conditions but two initial conditions on f and one initial condition each on g, θ and f are known. However the values of f', g, θ and f are known at . These four end conditions are utilized to produce four unknown initial conditions at η=0 by using shooting technique. The most crucial factor of this scheme is to choose the appropriate finite value of . In order to estimate the value of , we start with some initial guess value and solve the boundary value problem consisting of Eqs. (13)-(17) to obtain f''(0), g'(0), θ'(0) and f'(0). The solution process is repeated with another large value of until two successive values of f''(0), g'(0), θ'(0) and f'(0) differ only after desired significant digit. The last value of is taken as the final value of for a particular set of physical parameters for determining velocity components f'(η), g(h), temperature θ(η) and concentration f(η) in the boundary layer. After knowing all the nine initial conditions, we solve this system of simultaneous equations using fifth-order Runge-Kutta-Fehlberg integration scheme with automatic grid generation scheme which ensures convergence at a faster rate. The value of greatly depends also on the set of the physical parameters such as Magnetic parameter, Hall parameter, Prandtl number, thermal radiation parameter, Lewis number, radiation parameter and chemical reaction parameter,convective heat transfer constant so that no numerical oscillations would occur. During the computation, the shooting error was controlled by keeping it to be less than 10-6.

4. SKIN FRICTION, NUSSELT NUMBER AND SHERWOOD NUMBER

The local skin-friction coefficient C_{fxz}, the local Nusselt number *Nu* and the local Sherwood number *Sh* defined by

$$C_{fx} = \frac{\tau_w}{\mu b x\sqrt{\frac{b}{v}}} = f''(0), C_{f_z} = g'(0) \tag{20}$$

$$\text{where } \tau_w = \mu\left(\frac{\partial u}{\partial y}\right)_{y=0} = \mu b x\sqrt{\tfrac{b}{v}}\, f''(0), Nu = \frac{\dot{q}_w}{k_f\sqrt{\frac{b}{v}}(T_w - T_\infty)} \tag{21}$$

$$\text{where } \quad q_w = -k_f\left(\frac{\partial T}{\partial y}\right)_{y=0} = -k_f\sqrt{\tfrac{b}{v}}(T_w - T_\infty)\theta'(0) \text{ and}$$

$$Sh = \frac{m_w}{D_m\sqrt{\frac{b}{v}}(C_w - C_\infty)} = -\phi'(0) \tag{22}$$

$$\text{where } \quad m_w = -D_m\left(\frac{\partial C}{\partial y}\right)_{y=0} = -D_m\sqrt{\tfrac{b}{v}}(C_w - C_\infty)\phi'(0)$$

5. COMPARISON

The results of this paper are compared with the results of previous published paper of Shit and Haldar [28] as shown in Table 1 and the outcomes are in good concurrence.

Table 1a. Comparison of Nu and Sh at η=0 with Shit and Haldar [28] withh1=0,Nb=Nt=0,E1=0,□=0

M	Rd	γ	θr	Shit and Haldar [28] Results		Present Results	
				Nu(0)	Sh(0)	Nu(0)	Sh(0)
0.5	1	0.5	-2	-0.6912	0.6195	-0.69139	0.61945
1.5	1	0.5	-2	-0.6977	0.6543	-0.69799	0.65455
0.5	3	0.5	-2	-12.3751	0.9278	-12.3758	0.92778
0.5	1	1.5	-2	-0.6956	1.0959	-0.69599	1.09612
0.5	1	-0.5	-2	-0.6966	0.4898	-0.69699	0.49096
0.5	1	-1.5	-2	-0.6968	0.4245	-0.69701	0.42499
0.5	1	0.5	-4	-0.5974	0.4071	-0.59755	0.40782
0.5	1	0.5	-6	-0.6969	0.6253	-0.69699	0.62582

In the absence of activation energy(E1=0) the results are in good agreement with Gnanaprasunamba et al [13]

Table 1b: Comparison of E1=0 at □=0 with Gnanaprasunamba et al [13]

m	Rd	h1	θr	γ	Gnanaprasunamba et al [13] Results		Present results	
					Nu(0)	Sh(0)	**Nu(0)**	**Sh(0)**
0.5	0.5	0.1	-2	0.5	0.0687655	0.697745	**0.0687695**	**0.697749**
1.0	0.5	0.1	-2	0.5	0.0691822	0.723509	**0.0691912**	**0.723511**
1.5	0.5	0.1	-2	0.5	0.0673211	0.725529	**0.0673223**	**0.725533**
0.5	1.5	0.1	-2	0.5	-0.119867	0.974017	**-0.1198877**	**0.974019**
0.5	3.5	0.1	-2	0.5	-0.415966	1.578952	**-0.4159876**	**1.578955**
0.5	0.5	0.2	-2	0.5	0.0691278	0.720812	**0.0691289**	**0.720819**
0.5	0.5	0.3	-2	0.5	0.0690176	0.721081	**0.06901895**	**0.721089**

0.5	0.5	0.1	-4	0.5	0.0690314	0.721304	**0.0690356**	**0.721312**
0.5	0.5	0.1	-6	0.5	0.0690415	0.721867	**0.0690465**	**0.721871**
0.5	0.5	0.1	-2	1.0	0.0718984	0.766751	**0.0718999**	**0.766756**
0.5	0.5	0.1	-2	1.5	0.0751133	0.817945	**0.0751156**	**0.817955**
0.5	0.5	0.1	-2	-0.5	0.0604131	0.584771	**0.0604176**	**0.584788**
0.5	0.5	0.1	-2	-1.0	0.0589067	0.560792	**0.0589089**	**0.560799**
0.5	0.5	0.1	-2	-1.5	0.0548573	0.495979	**0.0548588**	**0.495982**

6. RESULTS AND DISCUSSION

The system of coupled non-linear Eqs. (13)-(17) together with the boundary conditions (15) and (16) have been solved numerically. In our present study the numerical values of the physical parameters have been chosen so that G, M, m, Rd, γ, nb,Nt,h1 and θr are varied over a range which is listed in the following figures. (cf. Watanabe and Pop [30],Salem [26], Shit and Haldar [28].Ozotop and Abu-Nada[23].

Figs.2a-9a represent the axial velocity f' and cross flow velocity g(h) which is induced due to the presence of the Hall effects. All these figures show that for any particular values of the physical parameters g reaches a maximum value at a certain high above the sheet and beyond which g(h) decreases gradually in asymptotic nature for different velocities of G, M, m, N, Rd, γ, Nb,Nt,θr,E1,□ ,n,h1 and Le.

Figs.2(a & b) represent $f'(\eta)$ and g(h) with Grashof Number G. It is found that the axial and cross flow velocity components enhances with increase in thermal buoyancy force in the flow region.An increase in G rises the temperature and reduces the nanoconcentration in the boundary layer (Figs.2(c & d)), respectively. The variation of axial velocity $f'(\eta)$ and g(h) with magnetic parameter M shows that the primary velocity(f') depreciates and cross flow velocity(g) enhances with increase in magnetic parameter M. The variation of temperature (θ) and nanoconcentration (□) with M shows that higher the Lorenz force, smaller the temperature and larger the nanoconcentration in the boundary layer. This is due to the fact that the thickness of the thermal decays and molecular boundary layers grows with M (Figs.2(c & d)) respectively.

Figs.3(a & b) shows that the axial and cross flow velocities increase with increase in Hall parameter (m).This is due to the fact that as m increases the Lorentz force which opposes the flow and leads to the degeneration of the fluid motion. The anomalous behaviour of θ with variation of m is observed due to the presence of the Hall Current and there by induces a cross flow velocity component g(η). For an increase in the Hall parameter (m) we noticed an enhancement in both the velocities in the flow region. From Figs.3(c & d), we find that an increase in the Hall parameter (m), results in a deprecation in the nanoconcentration and enhancement in temperature.With respect to buoyancy ratio(N) we find that when the molecular buoyancy force dominates over the thermal buoyancy force the velocities enhance while temperature upsurges and nanoconcentration decays with increasing values of buoyancy ratio(N)(figs.3a-3d).

Fgs.4a-4d show the variation of f',g,θ and □ with Brownian motion parameter(Nb) and thermophoresis parameter(Nt).The velocity components ,temperature enhance and the nanoconcentrationexperiences a depreciation with rising values of Nb/Nt in the flow region(figs.4a-4d).

Figs.5(a-d) represent the variation of velocity components,temperature and nanoconcentration with radiation parameter(Rd) and viscosity parameter(θr).It can be seel from the profiles higher the radiative heat flux smaller the axial and cross flow velocities. An increase in viscosity parameter(θr) increases the axial velocity and reduces the cross flow velocities.The temperature and nanoconcentrationaccelarate with higher values of θrand an increase in Rd depreciates the temperature and upsurges the nanoconcentrationin the entire flow region(figs.5a-5d). This may be attributed to the fact an increase in Rd,leads to a decay in the thickness of the thermal and growth in solutal boundary layers,while both thermal and solutal layers become thicker with higher values of viscosity parameter(□r).

Figs.6a-6d represent the effect of chemical reaction(γ)on the flow variables .The velocity components(f',g),nanoconcentrationdecay,temperature(□) upsurgesin degenerating chemical reaction case while in the generating case,f ',g,□ augment,□ decays in the flow region(figs.6a-6d).

The effect of activation energy and temperature difference ratio(□)on flow variables can be seen from figs.7a-7d.Higher the activation energy parameter(E1)larger the velocities,nanoconcentration(□) and smaller the temperature in the flow region.This is due to the fact that increase in E1 grows the thickness of the momentum,solutal boundary layers and decays the thermal boundary layer thickness.

The influence of newtonian cooling (h1)/index parameter(n) on flow variables can be seen from figs.8a-8d.From the profiles we notice an acceleration in the velocities,temperature and reduction in the nanoconcentration in the flow region.This may be attributed to the fact that the thickness of the momentum ,thermal boundary layers grow while the solutal layer decays with rising values of convective heat transfer constant(h1)(figs.8a-8d).

Figs.9a-9d depict the variation of flow variables f',g, □and □ with Lewis number(Le). It is found that the axial and cross flow velocities,nanoconcentrationdepreciate with increase in Le.An increase in Lewis number(Le) reduces the velocioties,nanoconcentrationand reduces the temperature in the entire flow region(figs.9a-9d).

The variation of Skin friction coefficients(Cfx,Cfz),Nusselt and Sherwood numbers(Nu,Sh) on the wall(η=0) with different parameters is exhibited in table.2.It is found that an increase in Grashof number (G)/Hall parameter(m)/Brownian motion (Nb)/Thermophoresis(Nt) reduces the Skin friction components(Cfx) , Nusselt number(Nu) and enhanesCfz and Sherwood number(Sh) on the wall(□=0).Higher the Lorentz force larger Cfx,Cfz and smaller the Nusselt and Sherwood number on the wall.When the molecular buoyancy force dominates over the thermal force largerCfx, Cfz,Nu and smaller Sh on the wall when the buoyancy forces are in the same direction.With reference to the radiation parameter(Rd) we find that an increase in Rd reduces Cfz and Sh,enhancesCfx,Nu at the wall h=0.An increase in variable viscosity parameter(θr) decays Cfx,Cfz,Nu and grows Sh on η=0.Increasing Activation energy parameter(E1) leads to a reduction in Cfx,Sh and growth inCfz,Nu on η=0.Cfx, reduces,Cfz,Nu and Sh enhance in the generating chemical reaction case while in degenerating chemical reaction casew(□>0)/temperature difference ratio(□)/index number(n)/Lewis number(Le), Cfx,Shenhance,Cfz,Nu decays on the wall. For higher values of convective heat transfer parameter(h1) leads to a rise in Cfz,Nu,Sh and decay in Cfx on the stretching wall(□=0).Thus the presence of the /activation energuE1)Newtonian cooling (h1)leads to a growth inNusseltand Sherwood number grows with h1 and decays with E1on the wall.

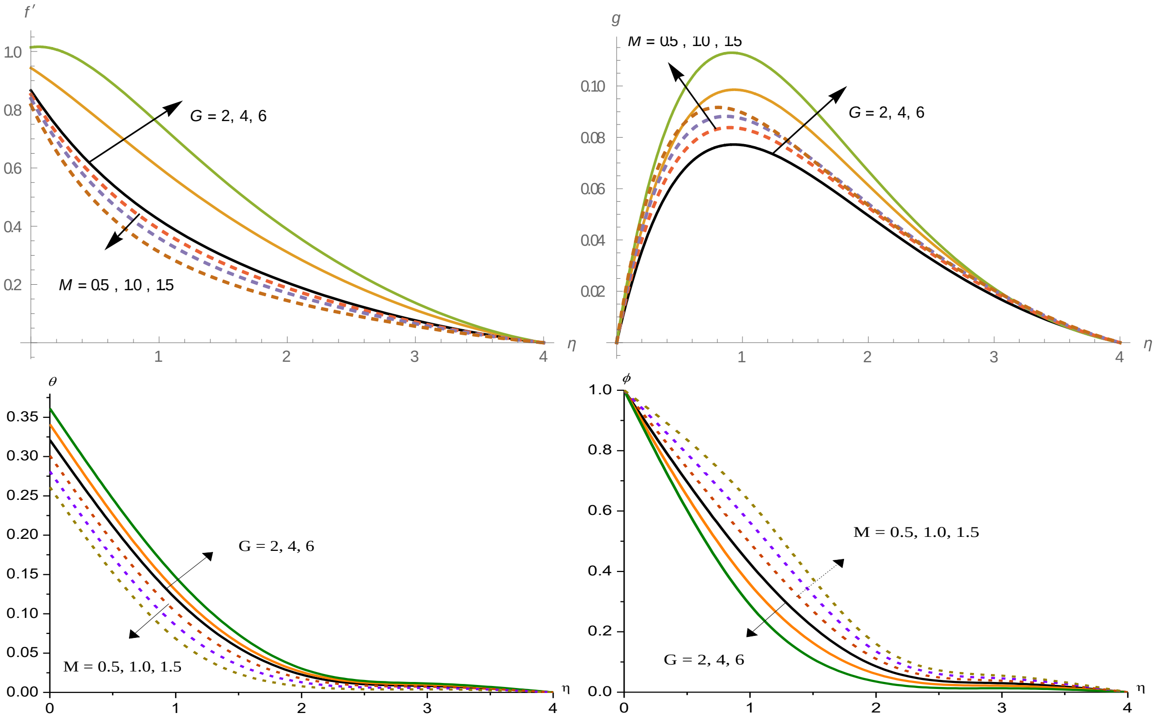

Figure 2: Variation of [a] Axial velocity (), [b]Cross flow velocity(g), [c] Temperature (□) and [d] Nano concentration (□) with G and M

m=0.5, N=0.5, Rd=0.5, Nb=0.1, Nt=0.1, h1=0.1, θr=-2, γ=0.5,E1=0.1,δ=0.1,n=0.2,Le=1

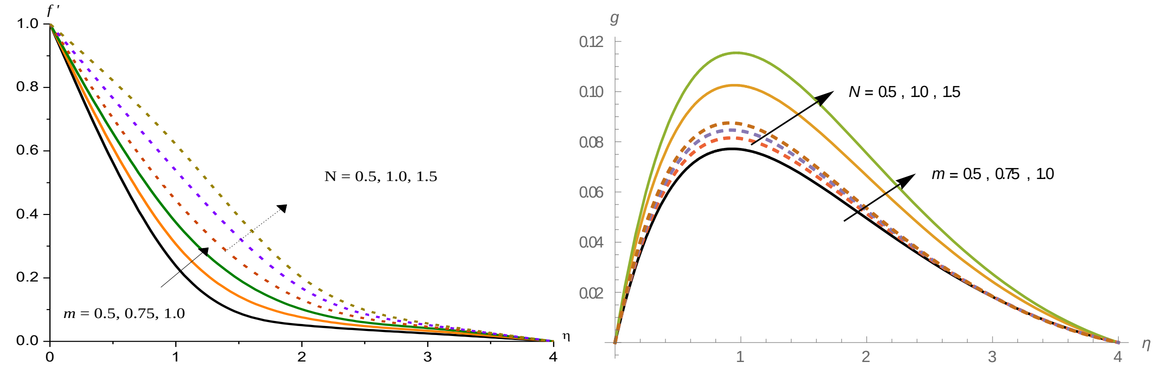

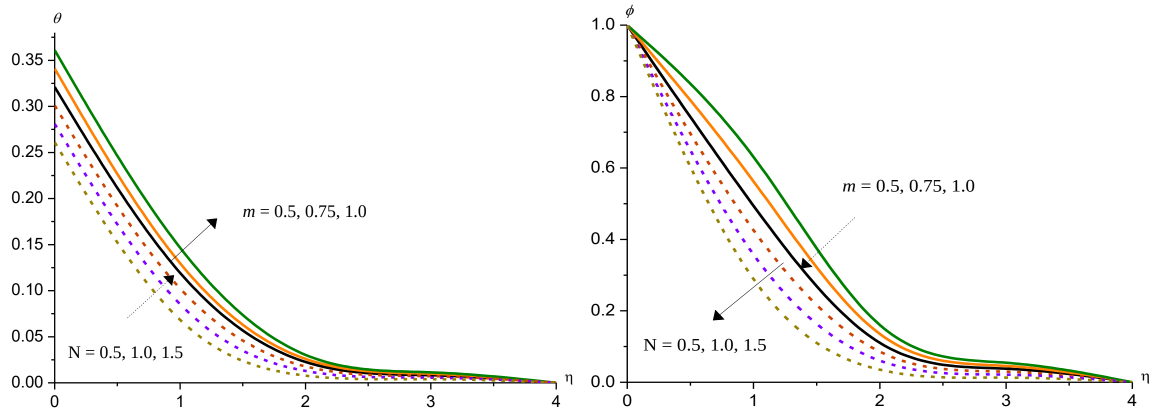

Figure 3: Variation of [a] Axial velocity (f'), [b]Cross flow velocity(g), [c] Temperature (θ) and [d] Nano concentration (ϕ)with m and N

G=2, M=0.5, Rd=0.5, Nb=0.1, Nt=0.1, h1=0.1, θr=-2, γ=0.5,E1=0.1,δ=0.1,n=0.2,Le=1

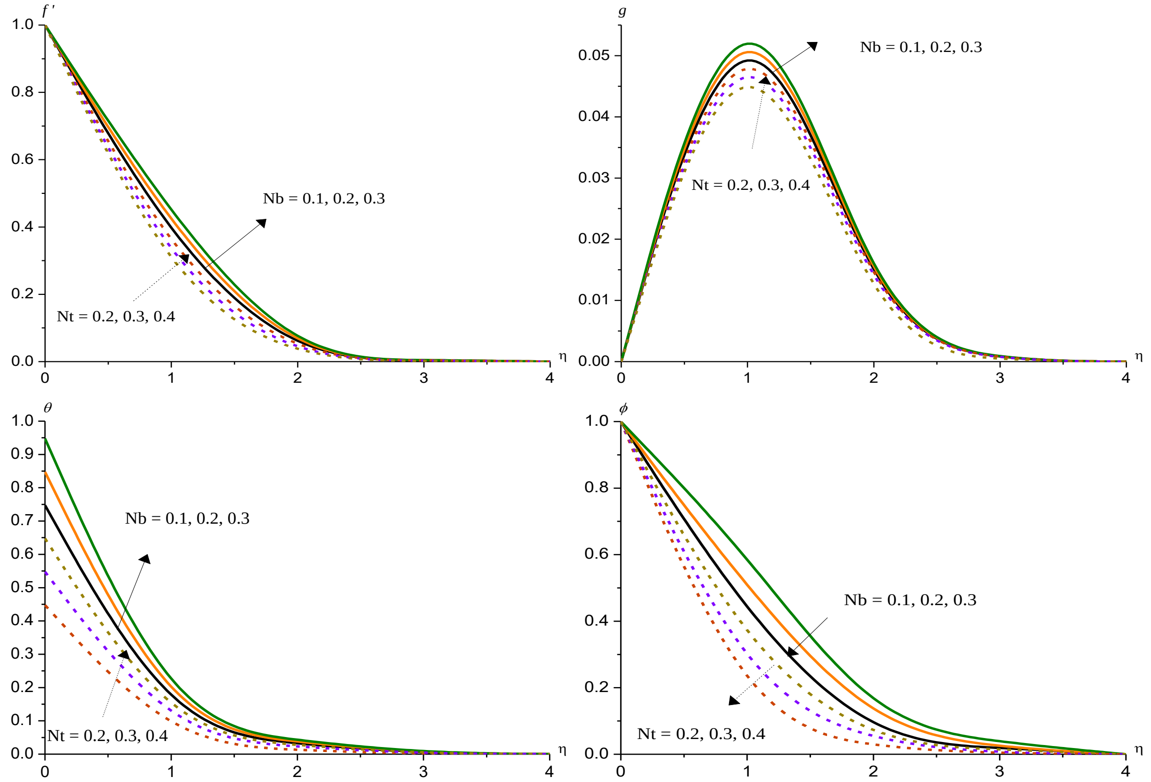

Figure 4: Variation of [a] Axial velocity (), [b]Cross flow velocity(g), [c] Temperature (□) and [d] Nano concentration (□) with Nb and Nt

G=2, M=0.5, m=0.5, N=0.5, Rd=0.5, h1=0.1, θr=-2,γ=0.5,E1=0.1,δ=0.1,n=0.2,Le=1

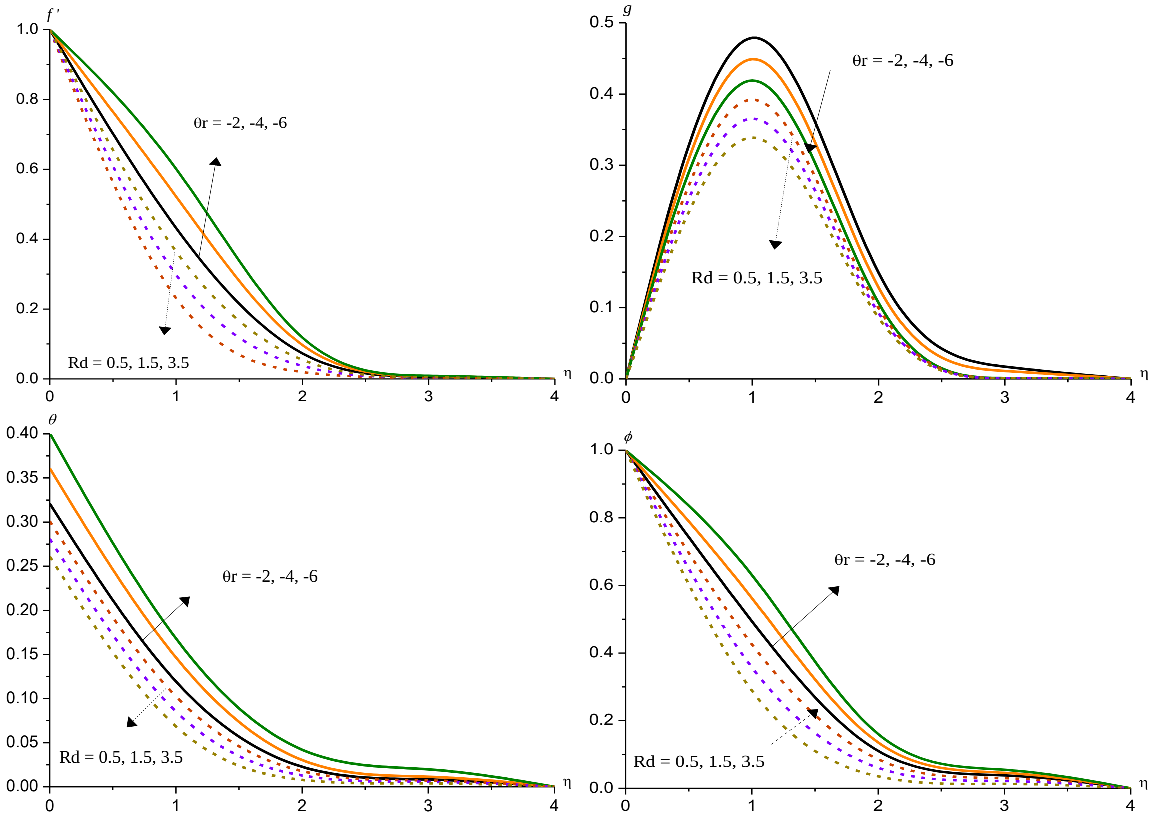

Figure 5: Variation of [a] Axial velocity(f'),[b]Cross flow velocity(g), [c] Temperature(θ) and [d] Nano concentration(ϕ)with θr and Rd

G=2, M=0.5,m=0.5,N=0.5,Nb=0.1,Nt=0.1,h1=0.1,γ=0.5,E1=0.1,δ=0.1,n=0.2,Le=1

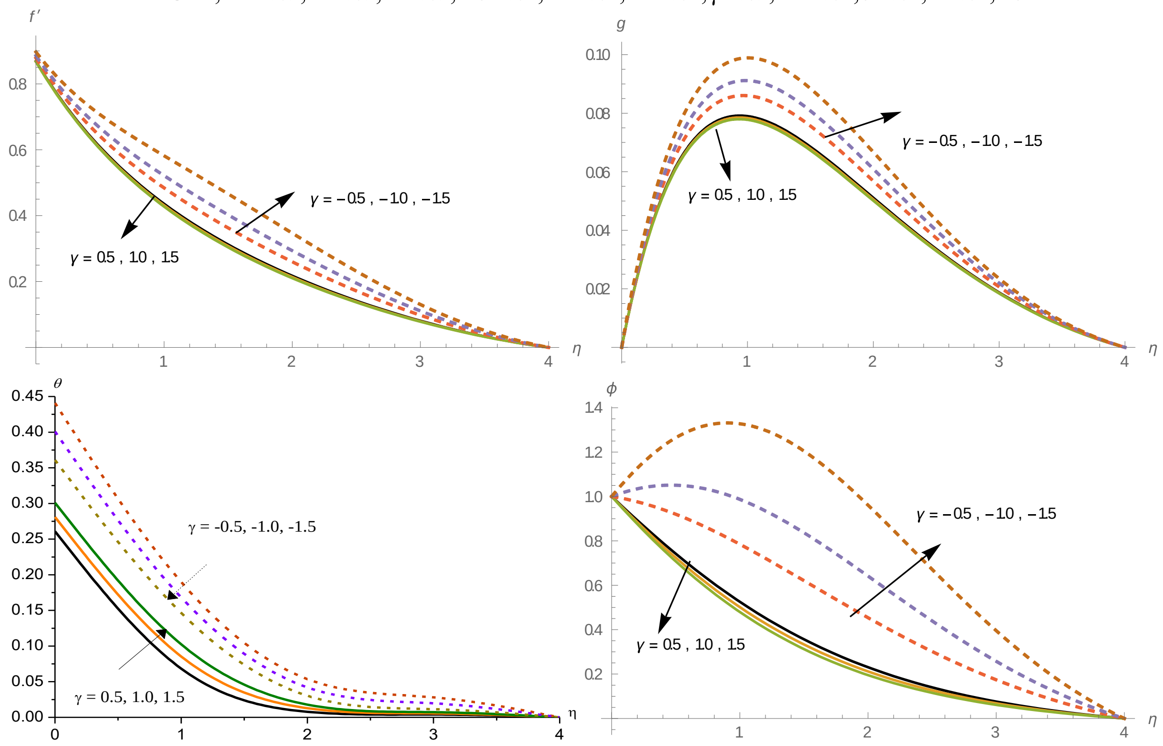

Figure 6: Variation of [a] Axial velocity (f'), [b]Cross flow velocity(g), [c] Temperature (θ) and [d] Nano concentration (ϕ)with γ

G=2, M=0.5, m=0.5, N=0.5, Rd=0.5, Nb=0.1, Nt=0.1, h1=0.1,θr=-2,n=0.2,Le=1

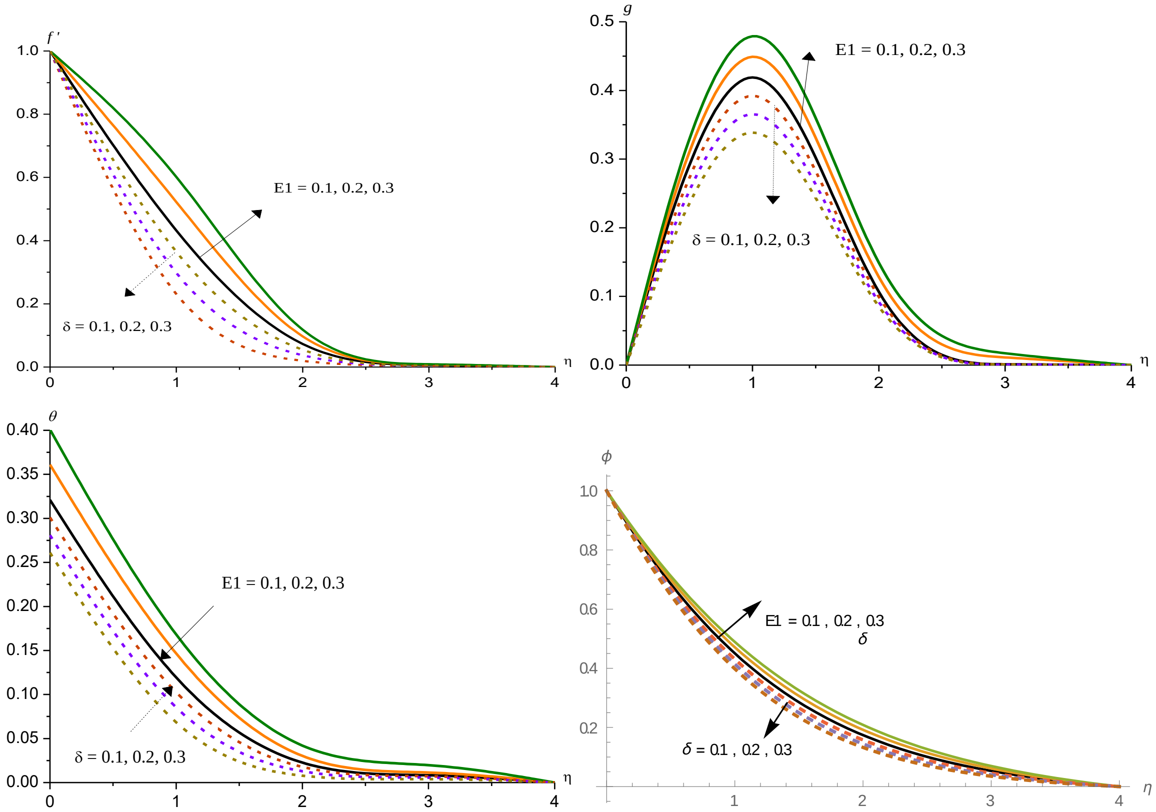

Figure 7: Variation of [a] Axial velocity (f'), [b]Cross flow velocity(g), [c] Temperature (θ) and [d] Nano concentration(ϕ)with E1 and δ
G=2, M=0.5, m=0.5, N=0.5, Rd=0.5, Nb=0.1,Nt=0.1,h1=0.1,θr=-2,γ=0.5,n=0.2,Le=1

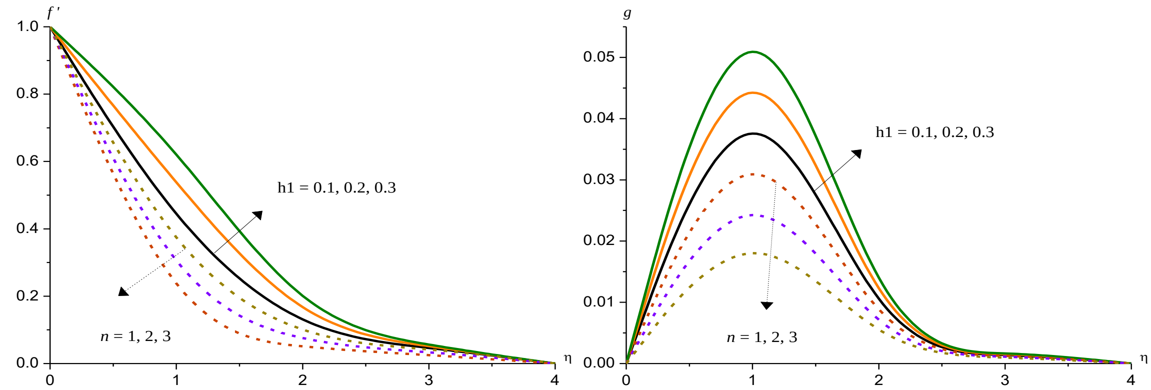

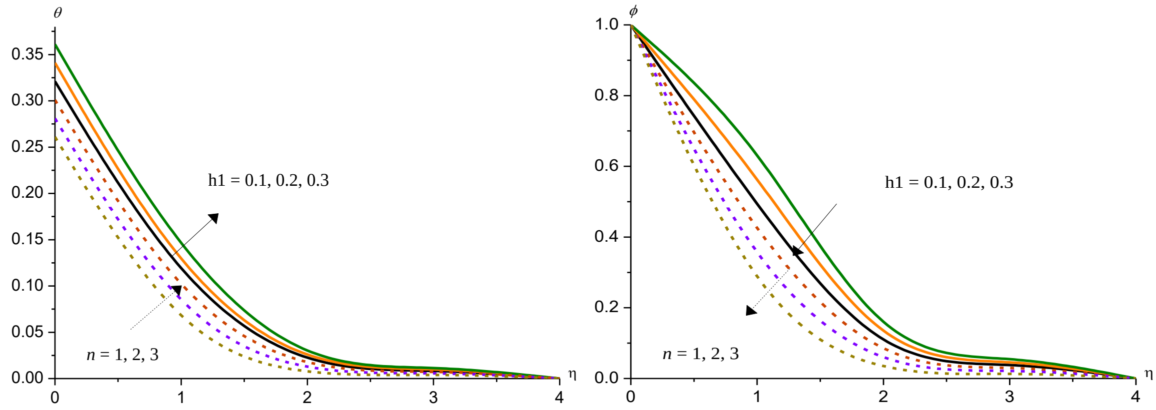

Figure 8: Variation of [a] Axial velocity (f'), [b]Cross flow velocity(g), [c] Temperature (θ) and [d] Nano concentration (ϕ)with h1 and n
G=2, M=0.5, m=0.5, N=0.5, Rd=0.5, Nb=0.1, Nt=0.1,θr=-2,θr=-2,γ=0.5,Le=1

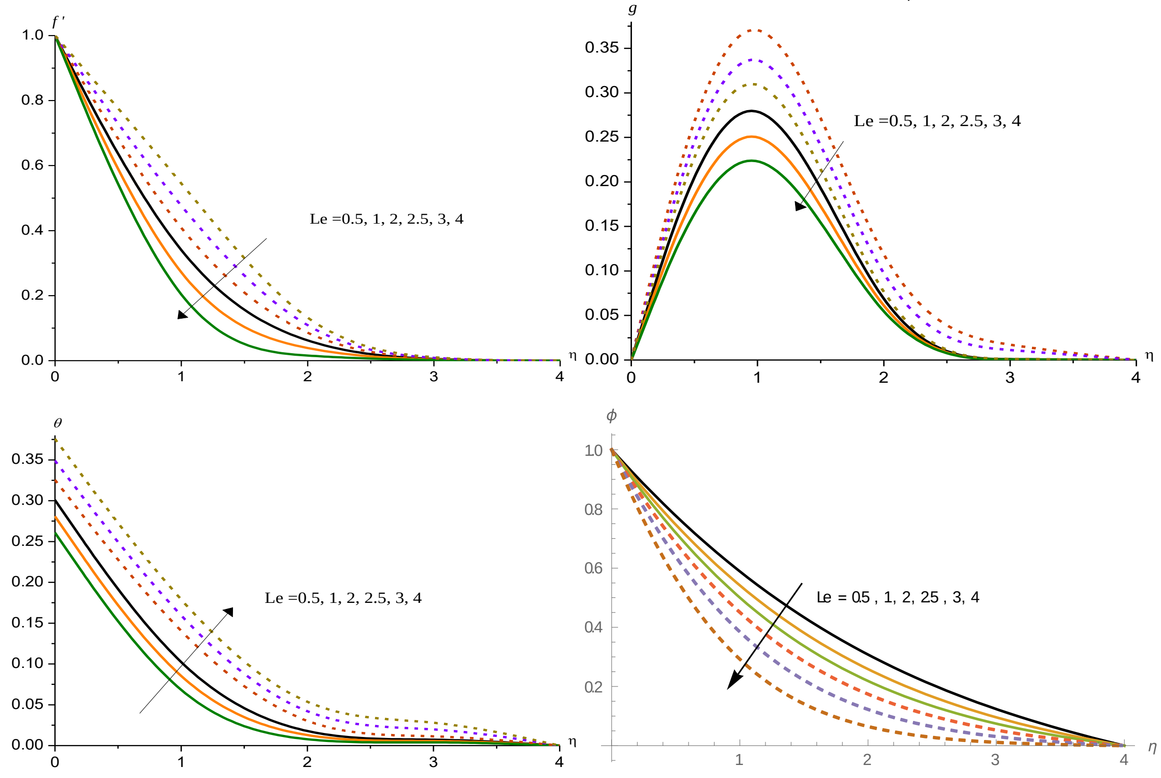

Figure 9: Variation of [a] Axial velocity (f'), [b]Cross flow velocity(g), [c] Temperature (θ) and [d] Nano concentration (ϕ)with Le
G=2, M=0.5, m=0.5, N=0.5, Rd=0.5, Nb=0.1, Nt=0.1, h1=0.1, θr=-2,γ=0.5,n=0.2

Table 2: Skin Friction ($Cf_{x,z}$), Nusslet number (Nu) and Sherwood Number (Sh) at η = 0

Parameter		$Cf_x(0)$	$Cf_z(0)$	Nu(0)	Sh(0)	**Parameter**		$Cf_x(0)$	$Cf_z(0)$	Nu(0)	Sh(0)
G	2	-0.668452	0.217874	0.110445	0.708851	Nb	0.1	-0.668454	0.217874	0.110445	0.708851
	4	-0.283562	0.265552	0.110423	0.748148		0.2	-0.667231	0.218267	0.109934	0.708906

	6	0.070363	0.302932	0.110419	0.781305		0.3	-0.665756	0.218657	0.109421	0.709045
M	0.5	-0.737588	0.248992	0.110447	0.701736	Nt	0.2	-0.668196	0.217957	0.110286	0.710638
	1.0	-0.806831	0.276844	0.110445	0.694747		0.3	-0.667998	0.218025	0.110113	0.713229
	1.5	-0.917714	0.315951	0.110455	0.683913		0.4	-0.667892	0.218066	0.109949	0.716159
m	0.5	-0.668453	0.217874	0.110445	0.708851	E1	0.1	-0.668435	0.217874	0.110445	0.708851
	0.75	-0.620405	0.279425	0.110443	0.713247		0.2	-0.664578	0.218823	0.110454	0.672207
	1.0	-0.582287	0.306287	0.110442	0.716913		0.3	-0.661186	0.219666	0.110462	0.640955
N	0.5	-0.576237	0.228402	0.110441	0.717432	δ	0.2	-0.672138	0.216988	0.110436	0.745125
	1.0	-0.504314	0.236267	0.110439	0.723937		0.3	-0.675297	0.216239	0.110429	0.777076
	1.5	-0.433785	0.243703	0.110437	0.730249		0.4	-0.678287	0.215541	0.110423	0.808123
Rd	1.5	-0.668944	0.217727	0.110645	0.708421	h1	0.1	-0.668454	0.217874	0.110445	0.708851
	3.5	-0.669214	0.217649	0.110753	0.708189		0.2	-0.591543	0.241183	0.155258	0.719278
	5.0	-0.669376	0.217599	0.110824	0.708044		0.3	-0.553846	0.252178	0.176197	0.724224
θr	-2	-0.668425	0.217874	0.110445	0.708851	n	1	-0.670102	0.217474	0.110441	0.724904
	-4	-0.649586	0.205922	0.110444	0.710516		2	-0.671706	0.217089	0.110437	0.740686
	-6	-0.642824	0.201821	0.110441	0.711123		3	-0.673264	0.216717	0.110434	0.756211
γ	0.5	-0.654226	0.221091	0.110475	0.547134	Le	0.5	-0.642537	0.224445	0.110513	0.480173
	1.0	-0.658763	0.220055	0.110465	0.596961		1.0	-0.651368	0.222149	0.110486	0.553846
	1.5	-0.662893	0.219119	0.110456	0.643678		2.0	-0.659134	0.220184	0.110467	0.621727

	-0.5	-0.607145	0.232077	0.110585	-0.089629							
	-1.0	-0.571925	0.240232	0.110674	-0.218777							
	-1.5	-0.514997	0.252813	0.110824	-0.705427							

7. CONCLUSIONS:

This analysis aims at investigating the effect of Activation energy, variable viscosity on convective heat transfer flow of nanofluid past a stretching surface which is maintained at Newtonian cooling. From the profiles we find that the higher the Hall parameter(m), buoyancy ratio(N), variable viscosity parameter(θr),Brownian motion parameter(Nb),thermophoresis parameter(Nt),activation energy(E1) larger the velocities., smaller the concentration. The velocities, temperature grow, concentration decays with rise in convective heat transfer constant(h1) The velocities, temperature rise with Brownian motion parameter (Nb) and thermophoresis (Nt). Nusselt number decrease with Hall parameter(m)/viscosity parameter(θr)/Nb/Nt and reduces with higher values of Rd/E1/h1.The rate of mass transfer (Sh) enhances with m/θr/Nb/Nt and reduces with increase in Rd/E1.The effect of activation energy is to reduce the Cfx,Sh and enhance Cfz,Nu on the wall(η=0).

8.REFERENCES

[1]. Abo-Eldahab EM, Salem AM. Hall effects on MHD free convection flow of a non-Newtonian power-law fluid at a stretching surface. Int. Commun. Heat Mass Transfer,V.31, pp:343-5 (2004).

[2]. Alam MS, Rahman MM, Sattar MA. Transient magnetohydrodynamic free convective heat and mass transfer flow with thermophoresis past a radiate inclined permeable plate in the presence of variable chemical reaction and temperature dependent viscosity. NonlinearAnal. Modell. Control, V.14(1), pp:3-20(2009).

[3]. Ali ME. The effect of variable viscosity on mixed convection heat transfer along a vertical moving surface. Int. J. Therm. Sci., V.45(1), pp:60-9 (2006).

[4]. Amitosh Tiwari : : activation energy impacts on hydromagnetic convective heat transfer flow of nanofluid past a surface of vertical wavy with variable properties, *International Journal of Computer Applications (0975 – 8887)* (2023)*Volume 184 – No. 50,* www.ijcaonline.org

[5]. Anjali Devi S.P. and Mekala S. (2019): Role of Brownian Motion and Thermophoresis Effects on Hydromagnetic Flow of Nanofluid Over a Nonlinearly Stretching Sheet with Slip effects and Solar Radiation *Int. J. of Applied Mechanics and Engineering, vol.24, No.3, pp.489-508,* DOI: 10.2478/ijame-2019-0031

[6]. Brewster MQ. *Thermal radiative transfer properties*. Wiley: New York, 1972.

[7]. Buongiorno. J (2006): Convective transport in nanofluids," ASME J Heat Tran vol.128, pp:240–250,

[8]. Chamkha AJ, Mansour MA, Aly AM. Unsteady MHD Free Convective Heat and Mass Transfer from a Vertical Porous Plate with Hall Current, Thermal Radiation and Chemical Reaction effects. International Journal for Numerical Methods in Fluids V.65, pp:432-47(2011).

[9]. Choi SUS, Eastman, JA : Enhancing thermal conductivity of fluids with nanoparticles, in. The Proceedings of the 1995, ASME, International mechanical Engineering Congress and Exposition, San Francisco, USA, ASME, FED 231/MD 66:, 99-105 (1995).

[10]. Devasena Y: effect of non-linear thermal radiation, activation energy on hydromagnetic convective heat and mass transfer flow of nanofluid in vertical channel with Brownian motion and thermophoresis in the presence of irregular heat sources, *World Journal of Engineering Research and Technology* (JERT) *wjert,* (2023), *Vol. 9, Issue 2, XX-XX,* ISSN 2454-695X, SJIF Impact Factor: 5.924, www.wjert.org

[11]. Dulal Pal, Netai Roy, Kuppalapalle Vajravelu,(2022): Thermophoresis and Brownian motion effects on magneto-convective heat transfer of viscoelastic nanofluid over a stretching sheet with nonlinear thermal radiation,International Journal of Ambient Energy Vol.43, Issu.1, P.413-424, https://doi.org/10.1080/01430750.2019.1636864

[12]. Falana, A., Ojewale, O.A. and Adeboje, T.B. (2016) Effect of Brownian Motion and Thermophoresis on a Nonlinearly Stretching Permeable Sheet in a Nanofluid. Advances in Nanoparticles, 2016, 5, 123-134, http://www.scirp.org/journal/anp, http://dx.doi.org/ 10.4236/anp.2016.51014.

[13]. Gnanaprasuna and ThippeswamyGonchigara : Effect of temperature gradient dependent heat source, secondary velocity on mixed convective flow of nanofluid through non-darcy porous medium with hall currents over an exponentially stretching surface with non-linear thermal radiation, *Journal of Advanced Research in Fluid Mechanics and Thermal Sciences* 102, Issue 2 (2023) 129-142, ISSN 2289-7879, https://semarakilmu.com. my/journals/ index.php/ fluid_mechanics_ thermal_ sciences/index
[14]. Gnanaprasunamba,K:Effect of Brownian motion and thermophoresis on nanofluid past a stretching surface w3ith variable viscosity and Newtonian cooling inspired by thermal radiation.,YMER ournal,Vol.21,Issue.4,pp.21-34(2022)
[15]. Kathyani,G and VenkataSubrahmanyam,P:Effect of dissipation on HD convective heat and mass transfer flow of thermally radiating nanofluid in vertical channel with activation energy and irregular heat sources.,MukthShabdJournal,ISSN No.2347 -3150,Scientific Journal;ISSN No:2347-3150, Vol.XII,Issue.III, March (2023) pp.433-441
[16]. KempannagariAnantha Kumar, VangalaSugunamma, Naramgari Sandeep, (2020) : Thermophoresis and brownian motion effects on mhdmicropolarnanofluid flow past a stretching surface with non-uniform heat source/sink, International Journal of Computational Thermal Sciences, Vol.12, Issue.1, pages 55-77.
[17]. Krishna M. V., Ahamad N. A., and Chamkha A. J., Hall and ion slip impacts on unsteady MHD convective rotating flow of heat generating/absorbing second grade fluid, 60, 845 (2021), DOI: 10.1016/j.aej.2020.10.013.
[18]. Mabood F, Ibrahim S.M., Khan W.A. (2016) : Framing the features of Brownian motion and thermophoresis on radiative nanofluid flow past a rotating stretching sheet with magnetohydrodynamics, Results in Physics 6, pp. 1015–1023 www.journals. elsevier.com/results-in-physics
[19]. Makinde OD. Laminar falling liquid film with variable viscosity along an inclined heated plate. Appl Math Comput V.175(1), pp:80-8(2006).
[20]. Mukhopadhyay S, Layek GC, Samad SA. Study of MHD boundary layer flow over a heated stretching sheet with variable viscosity. Int J Heat MassTransf, V.48(21-22), pp:4460–6(2005).
[21]. Nagasasikala M : Effect of activation energy on convective heat and mass transfer flow of dissipative nanofluid in vertical channel with Brownian motion and thermophoresis in the presence of irregular heat sources, *World Journal of Engineering Research and Technology* (JERT) *wjert, , Vol. 9, Issue 2,* (2023) *XX-XX,* ISSN 2454-695X, SJIF Impact Factor: 5.924, www.wjert.org
[22]. Netai Roy and Dulal Pal, : Influence of Activation Energy and Nonlinear Thermal Radiation with Ohmic Dissipation on Heat and Mass Transfer of a CassonNanofluid Over Stretching Sheet, Journal of Nanofluids, Vol. 11, No. 6, (2022) pp. 819–832, doi:10.1166/jon.2022.1882, www.aspbs.com/jon
[23]. Oztop. H. F and Abu-Nada. E (2008): Numerical study of natural convection in partially heated rectangular enclosures filled with nanofluids.,Int.J.Heat and Fluid Flow.,V.29,pp.1326-1336.
[24]. Prasad KV, Vajravelu K, Datti PS. The effects of variable fluid properties on the hydro-magnetic flow and heat transfer over a non-linearly stretching sheet. Int J ThermSci, V.49(3), pp:603-10(2010).
[25]. Rana. P and Bhargava R Flow and heat transfer of a nanofluid over a nonlinearly stretching sheet", Comm. Nonlinear Sci. Number Simulation, vol. 7, pp:212–226.
[26]. Salem AM. Variable viscosity and thermal conductivity effects on MHD flow and heat transfer in viscoelastic fluid over a stretching sheet. Phys Lett A; V.369(4), pp:315-22(2007).
[27]. Satya Narayana K and Ramakrishna G N : Effect of variable viscosity, activation energy and irregular heat sources on convective heat and mass transfer flow of nanofluid in a channel with brownian motion and thermophoresis, *World Journal of Engineering Research and Technology* (WJERT), (2023)*, Vol. 9, Issue 2, XX-XX,* ISSN 2454-695X, SJIF Impact Factor: 5.924, www.wjert.org
[28]. Shit GC and Haldar R. Combined effects of Thermal Radiation and Hall Current on MHD Free-Convective Flow and Mass Transfer over a Stretching Sheet with Variable Viscosity. J Applied Fluid Mechanics; V.5, pp: 113-21 (2012).
[29]. Shobha K C and PatilMallikarjun B (2021) : Fully developed mixed convection in a vertical channel filled with nanofluids with heat source or sink, Palestine Journal of Mathematics (Palestine Polytechnic University-PPU), Vol. 10 (Special Issue I), 29– 38.
[30]. Watanabe T, Pop I. Hall effects on magneto-hydrodynamic boundary layer flow over a continuous moving flat plate. ActaMechanica; V.108, pp:35-47 (1995).
[31]. Xi-Yan Tian, Ben-Wen Li, Ya-Shuai Wu, Jing-Kui Zhang. Chebyshev collocation spectral method simulation for the 2D boundary layer flow and heat transfer in variable viscosity MHD fluid over a stretching plate. International Journal of Heat and Mass Transfer, V.89, pp:829-37(2015).
[32]. Zahir Shah, PoomKumam&WejdanDeebani, Scientific Reports *(2020) 10:4402,* https://doi.org/10.1038/s41598-020-61125-9 www.nature.com/ scientificreports